Electronic Supplementary Material (ESI) for Nanoscale Horizons.

Chemical exfoliation of 1-dimensional antiferromagnetic nanoribbons from a non-van der Waals material

Mulan Yang,[a] Guangming Cheng,[b] Nitish Mathur,[a] Ratnadwip Singha,[a] Fang Yuan,[a] Nan Yao[b] and Leslie M. Schoop[a]

[a] *Department of Chemistry, Princeton University, Princeton, NJ 08544, United States.*
[b] *Princeton Materials Institute, Princeton, NJ 08544, United States.*

E-mail: lschoop@princeton.edu

We have performed preliminary experiments to show the applicability of our method to materials other than $KFeS_2$. We chose to exfoliate the compound $KSbS_2$ because it shares the same space group as $KFeS_2$ ($C2/c$) and has a similar chain motif. However, as seen in Fig. S1a, the chains in $KSbS_2$ are flatter than those in $KFeS_2$, which may lower its structural stability during the exfoliation process. Selected area electron diffraction patterns (SAEDs) of our preliminary results suggest that cleavage may occur along the same planes as in $KFeS_2$ (Fig. S1b). The SAEDs shown in Fig. S1c-d are indexed to the [010] and [100] zone axes, respectively, again matching those of $KFeS_2$. Thus, using the same reasoning, it is possible that the $KSbS_2$ nanostructures are formed by cleaving at the *ac* and *bc* planes. However, we cannot be certain that this is the only cleavage mechanism because SAEDs from other axes are often seen as well, unlike in the case of $KFeS_2$. In addition, the measured d-spacings do not match as closely to the expected values (Table S1, S2), which may imply a more complex cleavage mechanism.

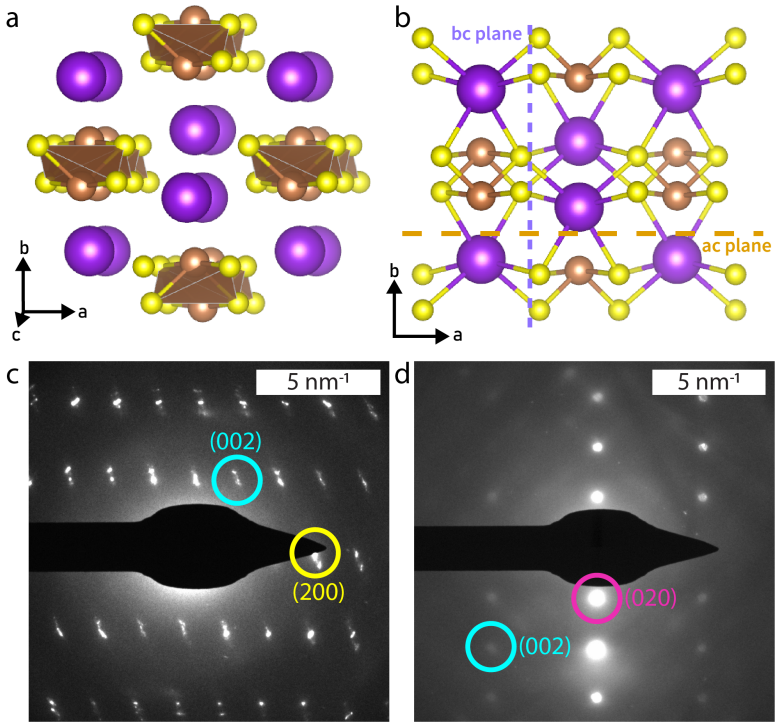

Figure S1: a) Structure of $KSbS_2$ highlighting its chain motif. b) Structure of $KSbS_2$ as seen from *c*-axis, showing the likely cleavage planes. c) SAED image of $KSbS_2$ nanostructure indexed to the [010] zone axis. d) SAED image of $KSbS_2$ nanostructure indexed to the [100] zone axis.

Plane	Theoretical (Å)	Measured (Å)	Difference (%)
(002)	2.92	2.94	0.93
(200)	3.73	5.50	47.37

Table S1: D-spacing measurements from a representative SAED pattern of $KSbS_2$ along the [010] zone axis.

Plane	Theoretical (Å)	Measured (Å)	Difference (%)
(002)	2.92	2.14	-26.7
(020)	4.48	4.47	-0.25

Table S2: D-spacing measurements from a representative SAED pattern of $KSbS_2$ along the [100] zone axis.

To obtain the exfoliated nanostructures shown in Fig. S2a-c, bulk $KSbS_2$ was sonicated in a 1:1 mixture of water and ethanol at 1 mg/mL for 120 min, 90 min, and 180 min, respectively. We then used energy-dispersive X-ray spectroscopy (EDX) (Fig. S2d-f) to confirm that the expected elements are homogeneously distributed throughout the nanostructures. From this data, we can be more confident that there is no significant phase change caused by, for example, a complete loss of K^+ ions.

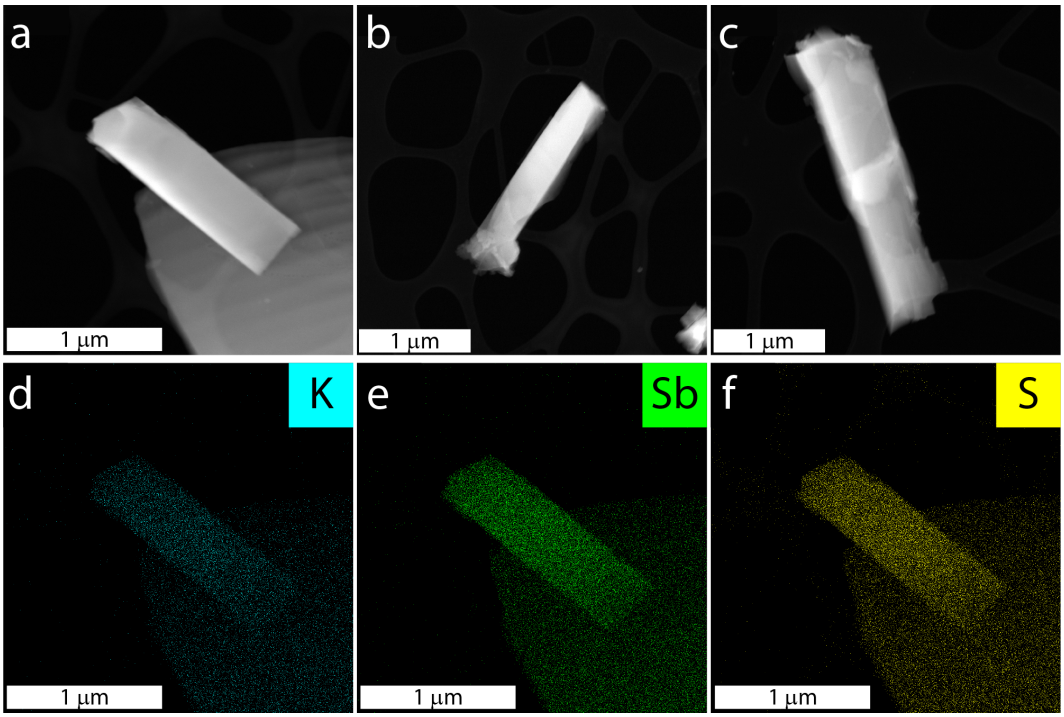

Figure S2: a-c) Nanostructures obtained after sonicating bulk $KSbS_2$ in a 1:1 mixture of water and ethanol. d-f) EDX maps of nanostructure in panel (a), showing the distribution of K, Sb, and S, respectively.

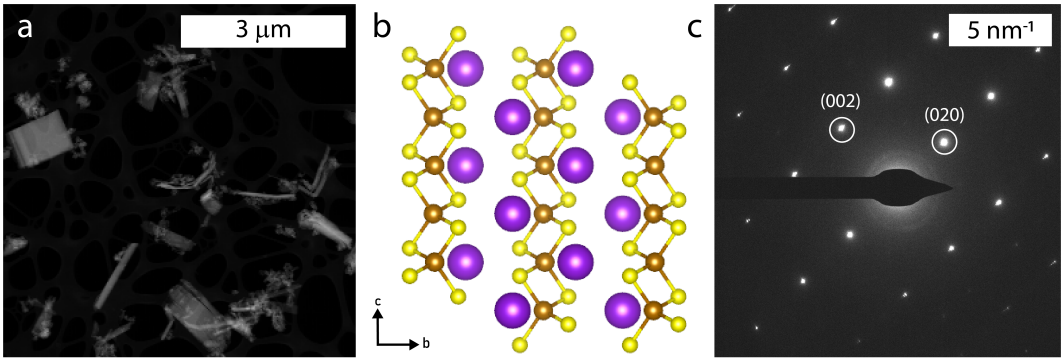

Figure S3: a) HAADF-STEM image of nanoribbons and nanosheets from the sample used for XRD. b) Structure of $KFeS_2$ as seen from a-axis. c) SAED image of nanoribbon indexed to the [100] zone axis. The (002) d-spacing matches the expected value, but the (020) d-spacing does not.

Plane	Theoretical (Å)	Measured (Å)	Difference (%)
(002)	2.48	2.43	-2.07
(200)	3.25	3.17	-2.44

Table S3: D-spacings measured from SAED pattern of "long nanoribbon" seen in Fig. 2d in the main text. This is a representative measurement of an SAED pattern along the [010] zone axis.

Plane	Theoretical (Å)	Measured (Å)	Difference (%)
(002)	2.48	2.56	2.54
(020)	5.65	3.14	-45.1

Table S4: D-spacings measured from SAED pattern seen in Fig. S1c. This is a representative measurement of an SAED pattern along the [100] zone axis.

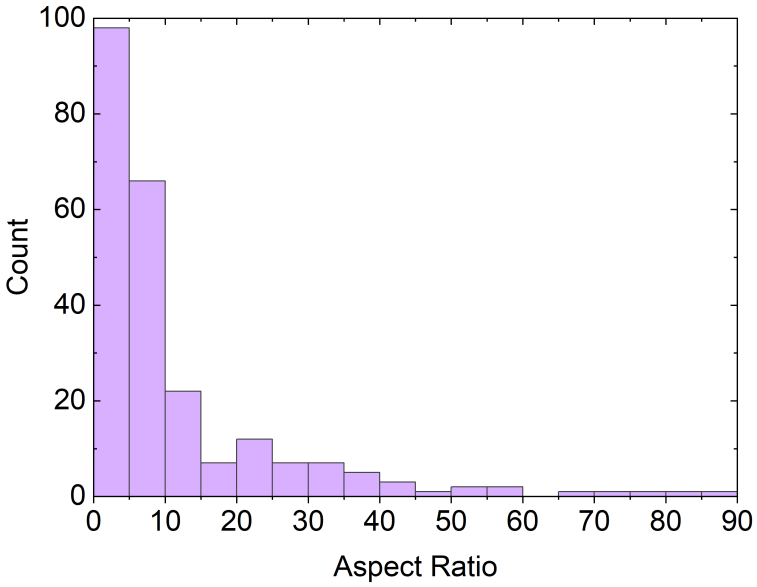

Figure S4: Histogram showing distribution of aspect ratios among the samples measured. The first bar (aspect ratios 0 - 5) represent the nanosheets; the rest are all considered nanoribbons.

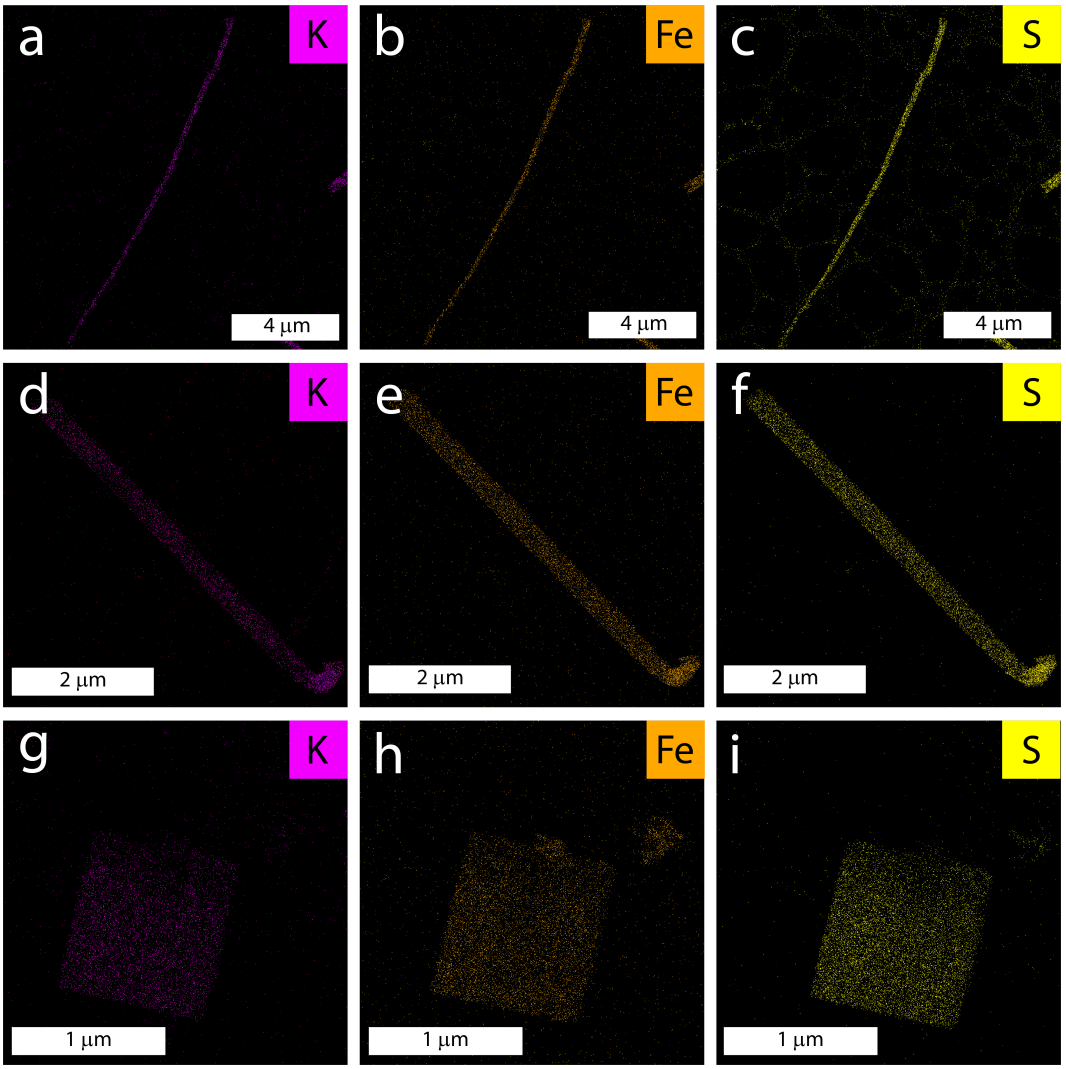

Figure S5: EDX maps corresponding to the a-c) long nanoribbon, d-f) nanoribbon, and g-i) nanosheet shown in Fig. 3.

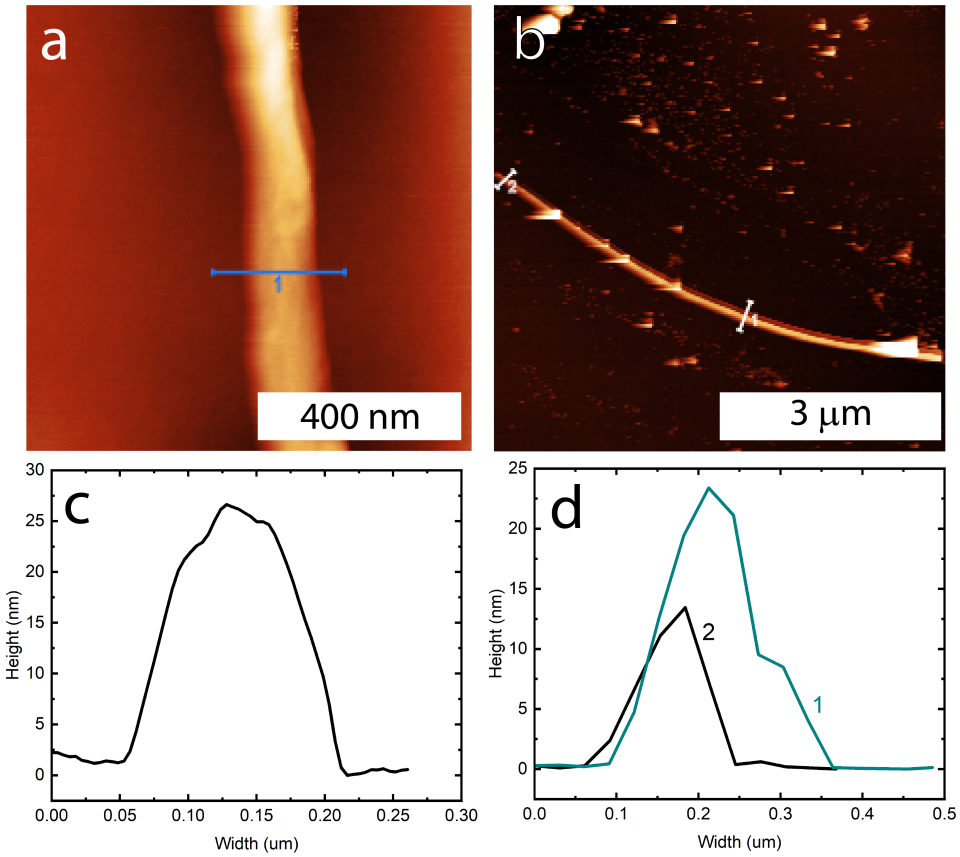

Figure S6: a,b) More nanoribbon samples measured by atomic force microscopy, with corresponding height profiles shown in c,d.

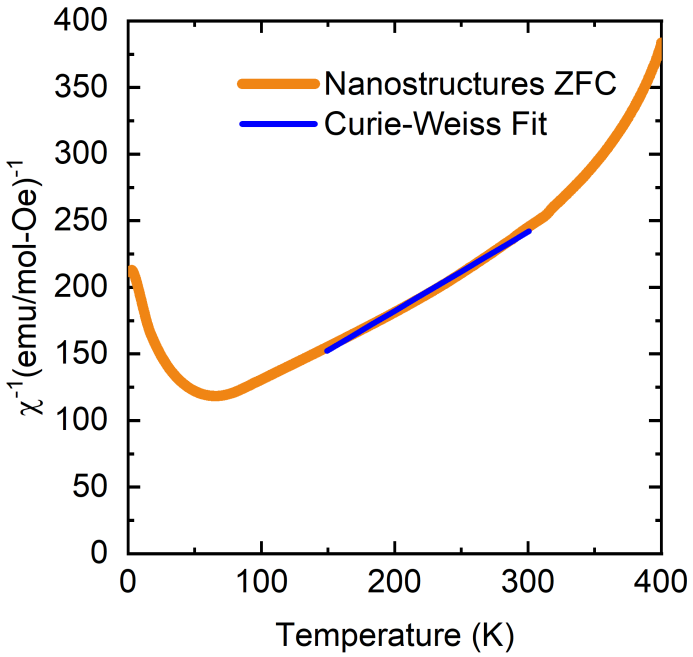

Figure S7: Curie-Weiss fit of intermediate temperature region of the magnetic susceptibility data of the exfoliated ensemble. The region >300 K curves dramatically, potentially due to interactions in a small bulk $KFeS_2$ impurity. Using these values, θ_{CW} = -108 K.